Archives of Virology

Identification and characterization of structural proteins of orchid fleck virus

Hideki Kondo[1], Takanori Maeda[2] and Tetsuo Tamada[1]

(1) Research Institute for Bioresources, Okayama University, 2-20-1, Chuo, Kurashiki 710-0046, Japan

(2) College of Bioresource Sciences, Nihon University, 1866 Kameino, Fujisawa, Kanagawa 252-8510, Japan

Running title: Structural proteins of OFV

H. Kondo (Corresponding author)

E-mail: hkondo@rib.okayama-u.ac.jp

Abstract Orchid fleck virus (OFV) has a bipartite negative-sense RNA genome with sequence similarities to plant rhabdoviruses. The non-enveloped bullet-shaped particles of OFV are similar to those of the internal ribonucleoprotein (RNP)-M protein structure of rhabdoviruses, but they are about half the size of typical plant rhabdoviruses. Purified preparations contained intact bullet-shaped and filamentous particles. The filamentous particles showed a tightly coiled coil structure or a coiled structure with a helical twist, which resembles the RNP complex of rhabdoviruses. OFV bullet-shaped particles were structurally stable in solutions containing 2% Triton X-100 and 0.8 M NaCl. Western blot analyses revealed that the bullet-shaped particles contained N, P and M proteins, while filamentous particles contained mainly N and P proteins. In addition, a small amount of the L protein was detected in both types of particles. Thus, the structural proteins of OFV have properties similar to those of rhabdoviruses, except that the particles are non-enveloped and are relatively resistant to a detergent treatment under high salt conditions.

Introduction

Members of the family *Rhabdoviridae* have a broad range of hosts, including humans, livestock, fish, plants, and insects. Rhabdovirus virions have an enveloped, bacilliform (most plant rhabdoviruses) or bullet-shaped (vertebrate rhabdoviruses) morphology, and measure 100–430 nm in length and 45–100 nm in diameter [33]. The rhabdovirus genome is a non-segmented and single-stranded negative-sense RNA, encoding at least five structural proteins: the nucleocapsid protein (or nucleoprotein) (N, Mr 47–62 × 10^3), phosphoprotein (P, Mr 20–30 × 10^3), matrix protein (M, Mr 20–30 × 10^3), glycoprotein (G, Mr 65–90 × 10^3) and RNA-dependent RNA polymerase (L, Mr 220–240 × 10^3) in the order 3' N-P-M-G-L 5'[33]. The viral RNA is tightly encapsidated by the N protein and this N–RNA complex, together with the P and L proteins, forms a helical ribonucleoprotein (RNP) complex that is essential for virus replication [29]. The M protein is responsible for condensation of RNP complexes into a skeleton-like structure (RNP-M core) during virion assembly, and G forms a virion spike [16, 33]. Plant rhabdoviruses encode at least one additional ORF, most commonly between the P and M genes [4, 8, 15, 24, 30], which has been thought to be involved in viral cell-to-cell movement in plants [4, 10, 15, 30]. Plant-infecting rhabdoviruses are classified into two genera, *Nucleorhabdovirus* and *Cytorhabdovirus,* in the family *Rhabdoviridae* [33].

Orchid fleck virus (OFV) has been proposed as the type species of a new genus *Dichorhabdovirus* [23]. However, the taxonomic position of OFV is still unclear because, despite having obvious physicochemical similarities to rhabdoviruses, the OFV genome is bipartite, while rhabdoviruses belong to the order *Mononegavirales*, negative-sense RNA viruses with non-segmented genomes [33]. OFV has non-enveloped bullet-shaped or bacilliform particles, 100−150 nm long and about 40 nm in diameter [1, 5], which resemble the condensed RNP-M core

of rhabdovirus virions [21]. OFV is transmitted by the false-spider mite *Brevipalpus californicus* [20]. In OFV-infected leaf tissue, the virus induces a characteristic, intranuclear, electron-lucent viroplasm [1, 17, 18, 23]. Virions can be seen scattered throughout the viroplasm and nucleus. A number of virions appear to be radially arranged as in a characteristic 'spoke-wheel'-like structure inside of the extrusion from the nuclear membrane toward the cytoplasm [1, 17, 18, 23].

OFV has a bipartite genome: RNA1 (6,413 nts) encodes the ORF1, ORF2, ORF3, ORF4 and ORF5 proteins, and RNA2 (6,001 nts) encodes ORF6 [21]. The ORF1, ORF5 and ORF6 proteins have significant similarities to the *N, G* and *L* gene products, respectively, of nucleorhabdoviruses [21]; therefore the respective gene products of OFV are referred to as N, G and L proteins. Indeed, Gosh et al. (2008) reported that the OFV N gene sequence clustered with that of nucleorhabdoviruses [6]. Similarly, the ORF2, ORF3 and ORF4 proteins are suspected to correspond to *P,* tentative movement protein and *M* gene products, respectively, of plant rhabdoviruses, but there were no significant similarities among the corresponding proteins [21]. Thus, although OFV has a sequence similarity to nucleorhabdoviruses, it differs from rhabdoviruses in having a bipartite genome and virions that are much smaller (about half the size) and lack a membrane. In this study, we identified four structural proteins constituting OFV bullet-shaped particles, and showed that these proteins have properties similar to those of plant rhabdovirus, except that structures of rhabdoviruses are not stable in detergent and under a high salt condition.

Materials and methods

Partial purification procedures

The original OFV isolate (So) was propagated in *T. expansa* in a glasshouse [19, 21]. OFV particles

were partially purified with two procedures. The first standard purification protocol was based on that described by Jackson and Wagner [13]. OFV-infected leaves were ground in a Waring blender in 4 volumes (w/v) of extraction buffer (100 mM Tris−HCI, pH 8.4, 10 mM $MgCI_2$, 1 mM $MnCl_2$, 40 mM Na_2SO_3). The homogenate was filtered through cheesecloth and centrifuged at 3,000 *g* for 10 min. The supernatant was layered on a discontinuous gradient consisting of two layers of 30% and 60% (w/v) sucrose in maintenance buffer (100 mM Tris-HCI, pH 7.5, 10 mM $MgCI_2$, 1 mM $MnCl_2$, 40 mM Na_2SO_3). After centrifugation for 1 h at 30,000 rpm at 4˚C in a Beckman SW28 rotor, the green band at the 30/60% sucrose interface was collected, and diluted with 0.5 volumes of maintenance buffer. The mixture was gently filtered through a Celite pad and centrifuged for 1 h at 30,000 rpm in a Beckman Ti 70 rotor. The resulting pellets were resuspended in distilled water.

The second purification was a detergent-treatment procedure modified from that described by Chang et al. [1]. OFV infected-leaves were ground in a Waring blender in 3 volumes (w/v) of 100 mM sodium phosphate buffer (pH 7.0) containing 0.1% thioglycolic acid. The homogenate was filtered through a double-layer of cheesecloth and centrifuged at 6,000 *g* for 10 min at 4˚C. Triton X-100 was added to the supernatant to a final concentration of 1% and stirred for 15 min. Polyethylene glycol (PEG) 6000 was added to the mixture to a final concentration of 6% and stirred for 1 h at 4˚C. The mixture was centrifuged at 6,000 *g* for 20 min at 4˚C. The pellet was resuspended in 10 mM sodium phosphate buffer (pH 7.0). The aqueous phase was centrifuged for 30,000 rpm in a Beckman Ti 70 rotor through a 25% sucrose cushion. The resulting pellets were resuspended in distilled water.

Purification by sucrose density and CsCl gradient centrifugations

Partially purified preparations were loaded on a 10–40% sucrose density gradient prepared in 10 mM sodium phosphate buffer (pH 7.0) and centrifuged for 1 h at 30,000 rpm at 4˚C in a Beckman

SW41 rotor. The light-scattering bands were collected from the gradient and pelleted by ultracentrifugation. The final pellet was resuspended in distilled water.

Partially purified OFV particles were loaded on a 20–40% cesium chloride (CsCl) gradient prepared in 20 mM Tris–HCl (pH 8.0), 200 mM NaCl and centrifuged for 16 h at 30,000 rpm in a Beckman SW41 rotor. The light-scattering bands were collected from the gradient and were dialyzed against the same buffer without CsCl.

Electrophoretic analysis of viral RNA and proteins

Nucleic acids were extracted from purified OFV particles using 1 % sodium dodecyl sulfate (SDS) in the extraction buffer (100 mM NaCl, 10 mM EDTA and 50 mM Tris-HCl, pH 8.0) followed by phenol extraction and ethanol precipitation. Viral nucleic acids extracted from purified virions were separated on 1.7 % agarose horizontal submarine gels in MOPS/EDTA buffer (pH 7.0) containing 0.22 M formaldehyde .

Viral proteins were denatured in loading buffer, 50 mM Tris-HCl (pH 8.8), containing 2% SDS, 1% 2-mercaptoethanol, 10% sucrose and 0.01% bromophenol blue for 5 min at 100˚C. The samples were analyzed in discontinuous SDS-polyacrylamide gel electrophoresis (SDS-PAGE) [22] and were stained with Coomassie Brilliant Blue R-250 (CBB).

Expression and purification of recombinant proteins

For expression of hexa-histidine (His6)-tagged proteins, the pET-15b vector (Novagen, Madison, WI) was used. Specific primers containing a *Bam*HI site upstream of the ATG start codon of the ORF1 (N), or *Nde*I site of the ORF2, ORF3 and ORF4, and a *Bam*HI site downstream of the stop codon of the respective ORFs, were used for amplification of the distinct ORF1, ORF2, ORF3 and

ORF4 (Fig. 1). To express the sequences of the middle portion (Gm) of the ORF5 (G) protein and the N-terminal (Ln) portion of the L polymerase (ORF6) protein, nt 4,760−5,647 corresponding to aa 61–356 of the G protein, and nt 183–1067 corresponding to aa 1–295 of the L protein, respectively, were amplified using specific primer pairs containing an *Nde*I site (forward primer) or a *Bam*HI site (reverse primer) (Fig. 1). As templates for PCR, the respective cDNA clones encompassing the gene of interest [21] were used. The resultant DNA fragments were digested with the appropriate enzymes and cloned into *Bam*HI or *Nde*I/*Bam*HI-restricted pET-15b (Novagen) to generate pET-N, pET-2, pET-3, pET-4 pET-Gm and pET-Ln, respectively (Fig. 1). Recombinant proteins were expressed from *Escherichia coli* BL21(DE3) using the pET system (Novagen) according to the manufacturer's specifications. The N terminus of all recombinant proteins had 20–25 extra amino acid residues which encompassed the His6 tag. The recombinant proteins His-N, His-ORF2, His-ORF4 and His-Ln were purified by Ni^{2+}-affinity chromatography using a HisBind Purification Kit (Novagen).

Production of antiserum

Antiserum to OFV was produced by intramuscular injections of purified virus into a New Zealand white rabbit. The purified virus (approximately 1 mg/ml) from the major band fraction in sucrose gradients (Fig. 3a) was emulsified with Freund's incomplete adjuvant (Difco, Detroit, MI) (1:1, v/v) and injected five times at biweekly intervals. The serum was collected one week after the last injection. The purification procedures for production of antisera specific to each of the 55-kDa, 29-kDa and 23-kDa proteins were as follows. Total proteins from the purified virus were fractionated by SDS-PAGE. The stained gel bands corresponding to the structural proteins were excised and the proteins were extracted electrophoretically from the gels and precipitated with acetone. The resulting proteins (0.1−0.3 mg) were emulsified with TiterMax adjuvant (CytRx Co.,

Norcross, GA) (1:1, v/v) and injected intramuscularly into a BALB/c mouse 3 times at 4 week intervals. Antisera were collected 1 week after the last injection. An antiserum to the N-terminal portion of the L (Ln) protein was generated by immunizing a rabbit with the purified Ln protein as described above.

Western blot analysis

For immunodetection, protein samples were transferred electrophoretically from SDS-polyacrylamide gels to nitrocellulose membranes (NCM; Bio-Rad, Hercules, CA) at 60 V for 5 h in 25 mM Tris containing 192 mM glycine and 20% methanol [32] and the NCM was blocked with 1% bovine serum albumin (BSA). Electroblots were probed with rabbit antisera to OFV virions (1:1000) and Ln (1:200) or the mouse antisera (1:200–500) specific to each protein. Then the electroblots were reacted with alkaline phosphatase-conjugated goat anti-rabbit IgG or anti-mouse IgG. Nitro blue tetrazolium and 5-bromo-4-chloro-3-indolyl phosphate were added for color development.

Electron microscopy

For transmission electron microscopy examination, the purified viral particles were placed on collodion-coated, carbon-stabilized copper grids (200 mesh) before they were negatively stained with 2% (w/v) uranyl acetate or 2% (w/v) ammonium molybdate. All sample grids were examined with a Hitachi H-7100 electron microscope.

Results

Morphology of OFV particles and analysis of their structural proteins

Two purification methods were compared; one is a standard procedure for plant rhabdoviruses described by Jackson and Wagner [13] and the other is a detergent-treatment procedure that is described here. With either the standard or the detergent-treatment purification procedure, many non-enveloped bullet-shaped particles (Fig. 2A) and filamentous structures associated with the bullet-shaped particles (Fig. 2A, arrowheads) were observed in partially purified OFV preparations (before sucrose density gradient centrifugation) stained with uranyl acetate. Although a few enveloped particles were observed in OFV-infected cells in the previous studies [1, 23], no enveloped particle was observed in preparations with the standard purification procedure. When stained with ammonium molybdate, bullet-shaped particles were broken partially from the ends of particles and shorter than normal particles (Fig. 2B) and filamentous particles appeared in loosely coiled helical strands (Fig. 2B, arrowheads, and 2C).

In SDS-PAGE, three major polypeptides with molecular masses of approximately 55 kDa, 29 kDa and 23 kDa were detected from partially purified preparations obtained with the two purification procedures (Fig. 2D, lanes 3 to 6). Western blot analysis revealed that the 55-kDa, 29-kDa and 23-kDa proteins strongly reacted with the antiserum to OFV virion (anti-OFV serum) (Fig. 2D, lanes 9–12). No staining was visualized in control experiments in which the preimmune serum was used in combination with the goat anti-rabbit IgG (data not shown). These results indicated that OFV particles contain at least three proteins and are stable in detergents such as Triton X-100 .

After sucrose density gradient centrifugation, one major band (Fig. 3A MaB) and one minor band (Fig. 3A MiB) were found at the lower and upper parts of the gradient, respectively. The preparation of the MaB fraction contained non-enveloped bullet-shaped particles of approximately

45–50 × 100–110 nm (Fig. 4A, 4B left). When 80 particles were examined for morphology and dimensions, most particles were uniformly bullet-shaped but a few particles were bacilliform (Fig. 4B right). These particles exhibited an orderly helix of about 25 turns with a pitch of approximately 4.5 nm (Fig. 4B). The MaB fraction contained a small number of disk-like subunits (about 45 nm in diameter) that were cross sections of virions (Fig. 4C). The morphology and structure of these particles closely resembled the internal RNP-M cores of rhabdovirus virions from which the outer membrane had been removed by detergent or enzyme treatment, even though the OFV particles are about the half of size of the cores of plant rhabdovirus virions [28, 34]. On the other hand, the preparation of the MiB fraction contained mainly filamentous particles about 20 nm wide and 200−500 nm long (Fig. 4D). The filamentous particles appeared to have a tightly coiled coil structure, and some particles were coil strands with a helical structure about 5 nm wide (Fig. 4E and 4F). A small number of disk-like subunits were also observed in this fraction. Both the MaB and MiB fractions contained genomic RNA1 and RNA2 (Fig. 3B).

SDS-PAGE and Western blot analysis showed that the bullet-shaped particles from the MaB fraction contained three proteins of 55 kDa, 29 kDa and 23 kDa (Fig. 3C: lanes 2 and 3; lanes 6 and 7), whereas the filamentous particles from the MiB fraction contained two proteins of 55 kDa and 29 kDa (Fig. 3C: lanes 4 and 5; lanes 8 and 9), although no or only a faint band of the 23-kDa protein was detected (Fig. 3C : lanes 4 and 5; lanes 8 and 9; data not shown). The 55 kD protein was abundant in both the MaB and MiB fractions (Fig. 3C). The sizes of the 55-kDa, 29-kDa and 23-kDa proteins were similar to those of N, P and M proteins of rhabdoviruses, respectively [33].

Western blot analysis revealed that the mouse antisera raised against the 55-kDa, 29-kDa and 23-kDa proteins reacted only in homologous combinations, indicating that these proteins were distinct polypeptides (Fig. 5A). These different proteins were also detected in extracts from OFV-infected *Chenopodium quinoa* leaves (Fig. 5B), but not in those from healthy *C. quinoa* leaves (Fig. 5B). The normal mouse serum did not reveal any staining (data not shown).

When inoculated onto *T. expansa* as described previously [21], the bullet-shaped particles from the MaB fraction but not the filamentous particles from the MiB fraction were infectious (data not shown).

Effect of NaCl and CsCl on stability of the OFV particles.

It is known that the helical nucleocapsid cores of rhabdoviruses are released from virions by treatment with nonionic detergents under high salt conditions (e.g., 0.5–0.8 M NaCl) [16, 26]. To determine if OFV bullet-shaped particles are converted to an extended helical structure under high salt conditions, the purified virus particles (1 mg/ ml) were incubated in 0.05 M Tris-HCl buffer (pH 7.4) containing 2% Triton X-100 and 0.8 M NaCl for 1 h and then centrifuged at 80,000 g for 1 h. The resulting pellets were resuspended in distilled water and were examined by electron microscopy. Most virus particles (70–80 %) were intact bullet-shaped forms (Fig. 6A), although some virus particles were degraded partially from one end or both ends of the particles (Fig. 6A, arrowheads). This indicated that OFV bullet-shaped particles are largely structurally stable under high salt conditions.

To examine the effect of CsCl on the stability of virus particles, partially purified particles were loaded onto a 20−40% (w/v) CsCl gradient in 20 mM Tris-HCl (pH 8.0) containing 200 mM NaCl and centrifuged for 16 h at 30,000 rpm. Near the bottom of the gradient a single major band was visible (Fig. 6D), which predominantly contained filamentous particles (Fig. 6B) but no bullet-shaped particles. Small numbers of partially disrupted particles and disk-like subunits were observed (Fig. 6C). In further experiments, the gradient was fractionated into 12 equal volumes which were then analyzed in a Western blot. In fraction 10 containing filamentous particles, a large amount of the 55-kDa protein, a small amount of the 29-kDa protein but no 23-kDa protein were detected (Fig. 6E). This fraction also contained the two genomic RNAs (data not shown). In

fractions 1 to 4, 29-kDa and 23-kDa proteins were detected (Fig. 6E). Some minor bands, presumably due to degradation or aggregation products of the OFV proteins, were detected in fractions 1 to 4 and 10 (Fig. 6E, asterisks). These results indicated that, during the CsCl gradient centrifugation, most of the bullet-shaped particles were converted to filamentous particles (N-RNA), from which the 29-kDa and 23-kDa proteins were also dissociated.

Analysis of prokaryotically expressed OFV proteins

OFV RNA1 encodes N, ORF2, ORF3, ORF4 and G proteins, and RNA2 encodes the L protein (Fig. 1) [21]. To confirm the identities of the 55-kDa, 29-kDa and 23-kDa proteins in the OFV genome, four entire ORFs (N, ORF2, ORF3 and ORF4), the middle part of ORF G and the 5'-terminal part of ORF L (Fig. 1) were cloned into pET 15b for protein expression in *E. coli.*

After induction of prokaryotic expression with IPTG followed by SDS-PAGE, the His6-tagged N, ORF2, ORF3, ORF4 and Ln proteins were expressed (Fig. 7A, lanes 2−5; and Fig. 7B−E, lane 2) and reacted with anti-His6 serum (data not shown). However, the expression product of the Gm protein was not detected in the bacterial lysate for unknown reasons (Fig. 7A, lane 6). In Western blot analysis, the anti-OFV serum reacted strongly with the expressed N, ORF2 and ORF4 proteins (Fig. 7a, lanes 9−11), but failed to react with the ORF3 and Ln proteins (Fig. 7A, lane 12; and data not shown). Moreover, the antisera to the 55, 29 and 23 kDa proteins reacted specifically with the N, ORF2 and ORF4 products, respectively (Fig. 7B−D, lane 5). The lysate from the bacteria expressing the ORF4 protein also contained a larger immunoreactive protein (28 kDa) (Fig. 7D, lane 5), which may be attributable to aberrant protein folding or protein modification in *E. coli* cells. Similar observations were made for the preparations of purified OFV particles (Fig. 5A; Fig. 7D, lane 4). These results indicated that the 55-kDa, 29-kDa and 23-kDa proteins corresponded to the N, ORF2 and ORF4 products, respectively.

A protein of high molecular weight (200 kDa) was detected in the bullet-shaped particles (and also in filamentous particles) when larger amounts of samples were loaded (Fig. 7E, lane 1; and data not shown). The 200-kDa protein reacted with an antiserum to the Ln protein (Fig. 7E, lane 4), indicating that ORF6 encodes the OFV L protein (212 kDa).

Discussion

We have shown here that the bullet-shaped particles of OFV are composed of four proteins, N, ORF2, ORF4, and L. The N protein was a main protein constituent of virus particles, while the ORF2 and ORF4 proteins were minor components of the particles. The particles contained only a small amount of the L protein. This structure and composition of OFV particles are similar to those of the RNP-M cores of rhabdoviruses [16, 33]. Together with the previous description of the OFV genome organization [21], these results indicate that the OFV ORF2 and ORF4 proteins should be referred to as P and M proteins, respectively, although they share no significant sequence similarities with the respective proteins of rhabdoviruses [21]. The notion that the structural proteins of OFV are similar to those of typical rhabdoviruses (i.e., vesicular stomatitis virus, rabies virus, sonchus yellow net virus) was also supported by protein-blotting overlay assays, providing evidence for physical interactions between the N and P proteins (unpublished data) [2, 3, 7, 31].

Generally, treatment of plant rhabdovirus particles with nonionic detergents results in the breakdown of condensed nucleocapsids into strands [12, 14]. In the case of OFV, however, most bullet-shaped particles remained largely intact following detergent treatment under high-salt conditions (e.g., 0.8 M NaCl). This indicates that the bullet-shaped particles of OFV are more resistant to a detergent treatment under high-salt conditions than plant rhabdovirus nucleocapsids. The filamentous particles that were released from the nuclei of infected plants and from intact

particles were collected from the upper part of the sucrose gradient. Most of the filamentous particles had a tightly coiled-coil structure, and some particles showed a coil structure with a helical twist. These filamentous particles contained N, P and L proteins, which together are thought to form an RNP complex such as that found in rhabdoviruses [16, 33]. Similar filamentous particles were also obtained by CsCl gradient centrifugation. In this case, many of the particles resembled an N-RNA complex with the P and L proteins removed [9, 11]. The fact that the filamentous particles did not contain the M protein suggests that the OFV M protein plays a role in maintaining the bullet-shaped conformation of virus particles [25, 26, 27]. Thus, the structure of bullet-shaped OFV particles resembles that of RNP-M cores of rhabdoviruses, except that the OFV particles have a higher structural stability.

Plant nucleorhabdoviruses have enveloped particles [15], whereas OFV particles appear to be non-enveloped [1, 5, 20]. It is known that the outer membranes of nucleorhabdoviruses are removed by a detergent treatment and the G protein forms the surface spikes of the mature membrane-bound particles [14, 15]. In the case of OFV, no outer membranes of the bullet-shaped particles were observed in partially purified preparations either with or without detergent treatment. Additionally, unlike the G proteins of nucleorhabdoviruses, the OFV G protein was not detected in virus particles by SDS-PAGE (Fig. 1). We reported previously that the OFV G protein has two potential glycosylation sites, whereas nucleorhabdovirus G proteins contain five to 10 potential glycosylation sites [21], suggesting that the smaller numbers of glycosylation sites in the OFV G protein may contribute to the lack of an outer membrane in OFV particles.

Acknowledgments We thank Koji Mitsuhata and Dr I Wayan Gara for their technical assistance, and Drs Narinobu Inouye, Ida Bagus Andika and Nobuhiro Suzuki for their helpful comments. This work was partially supported by a Grant-in-Aid for Scientific Research [KAKENHI] from the

Japanese Ministry of Education, Culture, Sport, Science and Technology, and by the Yomogi Inc.

References

1. Chang MU, Arai K, Doi Y, Yora K (1976) Morphology and intracellular appearance of orchid fleck virus. Ann Phytopathol Soc Jpn 42: 156-167
2. Chen M, Ogino T, Banerjee AK (2006) Mapping and functional role of the self-association domain of vesicular stomatitis virus phosphoprotein. J Virol 80: 9511–9518
3. Chenik M, Chebli K, Gaudin Y, Blondel D (1994) *In vivo* interaction of rabies virus phosphoprotein (P) and nucleoprotein (N): existence of two N-binding sites on P protein. J Gen Virol. 75: 2889–2896
4. Dietzgen RG, Callaghan B, Wetzel T, Dale JL (2006) Completion of the genome sequence of *Lettuce necrotic yellows virus*, type species of the genus *Cytorhabdovirus*. Virus Res 118: 16–22
5. Doi Y, Chang MU, Yora K (1977) Orchid fleck virus. CMI/AAB Description of Plant Viruses No. 183
6. Ghosh D, Brooks RE, Wang R, Lesnaw J, Goodin MM (2008) Cloning and subcellular localization of the phosphoprotein and nucleocapsid proteins of *Potato yellow dwarf virus*, type species of the genus *Nucleorhabdovirus*. Virus Res 135: 26–35
7. Goodin MM, Austin, J, Tobias R, Fujita M, Morales C, Jackson AO (2001) Interactions and nuclear import of the N and P proteins of sonchus yellow net virus, a plant nucleorhabdovirus. J Virol 75: 9393–9406
8. Heim F, Lot H, Delecolle B, Bassler A, Krczal G, Wetzel T (2008) Complete nucleotide sequence of a putative new cytorhabdovirus infecting lettuce. Arch Virol 153: 81–92
9. Heggeness MH, Scheid A, Choppin PW (1980) Conformation of the helical nucleocapsids of paramyxoviruses and vesicular stomatitis virus: reversible coiling and uncoiling induced by changes in salt concentration. Proc Natl Acad Sci USA 77:2631−2635
10. Huang YW, Geng YF, Ying XB, Chen XY, Fang RX (2005) Identification of a movement protein of rice yellow stunt rhabdovirus. J Virol 79: 2108–2114
11. Iseni F, Barge A, Baudin F, Blondel D, Ruigrok RW (1998) Characterization of rabies virus nucleocapsids and recombinant nucleocapsid-like structures. J Gen Virol 79: 2909–2919
12. Jackson AO (1978) Partial characterization of the structural proteins of sonchus yellow net virus. Virology 87: 172-181
13. Jackson AO, Wagner JDO (1998) Procedures for plant rhabdovirus purification, polyribosome isolation, and replicase extraction. Methods Mol Biol 81: 77−97
14. Jackson AO, Francki RIB, Zuidema D (1987) Biology, structure and replication of plant rhabdoviruses. In: Wagner RR (ed) The Rhabdoviruses. Plenum Press, New York, pp. 427‑ 508
15. Jackson AO, Dietzgen RG, Goodin MM, Bragg JN, Deng M (2005**)** Biology of plant rhabdoviruses. Annu. Rev Phytopathol 43: 623–660

16. Jayakar, HR, Jeetendra E, Whitt MA (2004) Rhabdovirus assembly and budding. Virus Res 106: 117–132
17. Kitajima EW, Blumenschein A, Costa AS (1974) Rodlike particles associated with ringspot symptoms in several orchid species in Brazil. Phytopathol Z 81: 280‐286
18. Kitajima EW, Kondo H, Mackenzie A, Rezende JAM, Glorla R, Gibbs A, Tamada T (2001) Comparative cytopathology and immunocytochemistry of Japanese, Australian and Brazilian isolates of Orchid fleck virus. J Gen Plant Pathol 67: 89‐96
19. Kondo H, Matsumoto J, Maeda T, Inouye N (1995) Host range and some properties of orchid fleck virus isolated from oriental *Cymbidium* in Japan. Bull. Res Inst Bioresour Okayama Univ 3: 151–161
20. Kondo H, Maeda T, Tamada T (2003) Orchid fleck virus: *Brevipalpus californicus* mite transmission, biological properties and genome structure. Exp Appl Acarol 30: 215–223
21. Kondo H, Maeda T, Shirako, Y, Tamada T (2006) Genome structure of Orchid fleck virus : a unique bipartite RNA genome that resembles nonsegmented negative stranded RNA viruses. J Gen Virol 87: 2413−2421
22. Laemmli UK (1970) Cleavage of structural proteins during the assembly of the head obacteriophage T4. Nature 227: 680-685
23. Lesemann D, Doraiswamy S (1975) Bullet-shaped virus-like particles in chlorotic and necrotic leaf lesions of orchids. Phytopathol Z 83: 27–39
24. Massah A, Izadpanah K, Afsharifar AR, Winter S (2008) Analysis of nucleotide sequence of Iranian maize mosaic virus confirms its identity as a distinct nucleorhabdovirus. Arch Virol 153: 1041–1047
25. Mebatsion T, Weiland F, Conzelmann KK (1999) Matrix protein of rabies virus is responsible for the assembly and budding of bullet-shaped particles and interacts with the transmembrane spike glycoprotein G. J Virol 73: 242–250
26. Newcomb WW, Brown JC (1981) Role of the vesicular stomatitis virus matrix protein in maintaining the viral nucleocapsid in the condensed form found in native virions. J Virol 39: 295–299
27. Newcomb WW, Tobin GJ, McGowan JJ, Brown JC (1982) *In vitro* reassembly of vesicular stomatitis virus skeletons. J Virol, 41: 1055–1062
28. Randles JW, Francki RI (1972) Infectious nucleocapsid particles of lettuce necrotic yellows virus with RNA-dependent RNA polymerase activity. Virology 50: 297−300
29. Rose JK, Whitt MA (2000) *Rhabdoviridae*: the viruses and their replication. In: Knipe DM, Howley PM, Griffin DE, Lamb RA, Martin MA, Roizman B, Straus SE, (eds) Fields Virology, 4th edition, Philadelphia, PA: Lippincott–Raven, pp. 1221–1240
30. Scholthof KB, Hillman BI, Modrell B, Heaton LA, Jackson AO (1994) Characterization and detection of sc4: a sixth gene encoded by sonchus yellow net virus. Virology 204: 279–288

31. Takacs AM, Das T, Banerjee AK (1993) Mapping of interacting domains between the nucleocapsid protein and the phosphoprotein of vesicular stomatitis virus by using a two-hybrid system. Proc Natl Acad Sci USA 90: 10375–10379
32. Towbin H, Staehelin T, Gordon J (1979) Electrophoretic transfer of proteins from polyacrylamide gels to nitrocellulose sheets: procedure and some applications. Proc Natl Acad Sci USA 76: 4350-4354
33. Walker PJ, Benmansour A, Dietzgen R, Fang RX, Jackson AO, Kurath G, Leong JC, Nadin-Davies S, Tesh RB, Tordo N. (2000) Family *Rhabdoviridae*. In: van Regenmortel MHV, Fauquet CM, Bishop DHL, Carstens EB, Estes MK, Lemon J, Maniloff SM, Mayo MA, McGeoch DJ, Pringle CR, Wickner RB, (eds) Virus Taxonomy–Seventh Report of the International Committee on Taxonomy of Viruses. Academic Press, San Diego, pp. 563–583
34. Ziemiecki A, Peters D (1976) The proteins of sowthistle yellow vein virus: characterization and location. J Gen Virol 32: 369-381

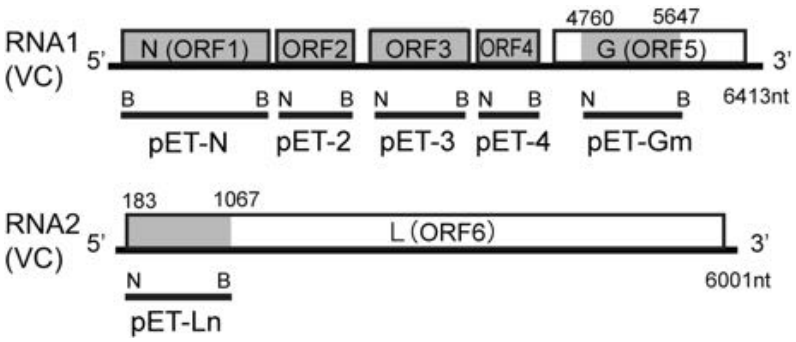

Fig. 1 Schematic representation of OFV RNA1 and RNA2. Boxes represent ORFs on the virus-complementary RNA (*VC*). Sizes and locations of PCR-generated fragments used for expression of viral proteins and Gm (middle part) and Ln (N-terminal part) proteins are shown. Primer-generated *Nde*I and *Bam*HI sites are indicated by N and B, respectively.

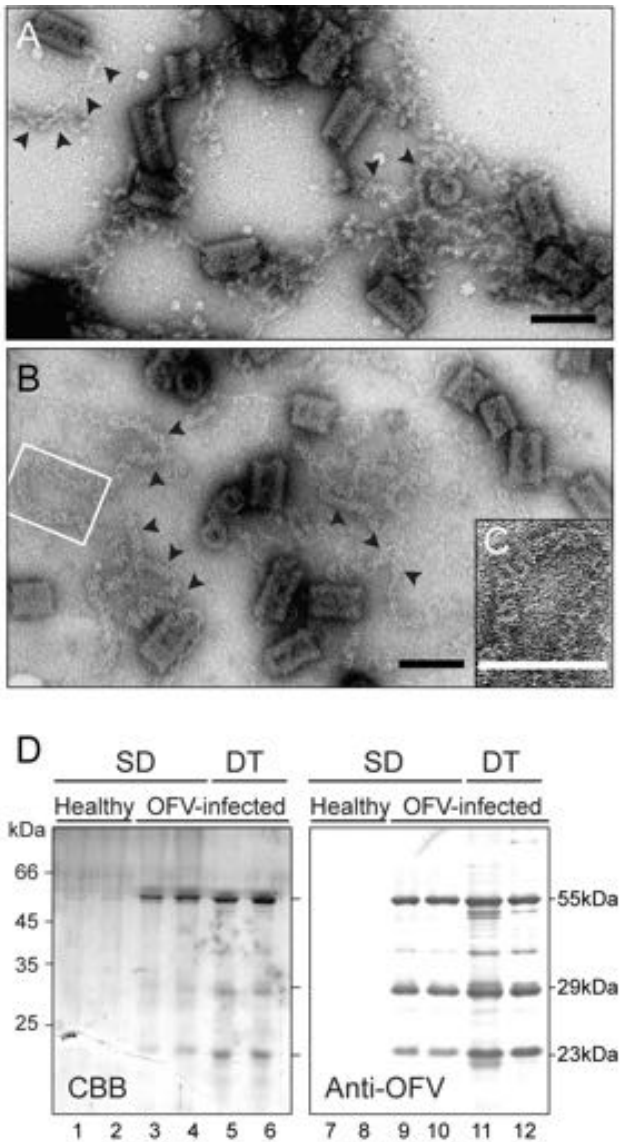

Fig. 2 OFV particles and analysis of their protein components. **A−C** Electron micrographs of the OFV particles purified by the detergent-treatment purification procedure. Samples were stained in uranyl acetate (A) or ammonium molybdate (B and C). *Arrowheads* indicate filamentous particles. The *bar* represents 100 nm. **C** An enlargement of the rectangle, showing a filamentous particle in B. **D** SDS-PAGE and Western blot analysis of partially purified preparations obtained from the standard (*SD*) and detergent-treatment (*DT*) purification procedures. Each sample was resolved in 12% SDS-PAGE gels followed by staining with Coomassie brilliant blue-R250 (*CBB*). The resolved proteins were transferred to nitrocellulose and reacted with rabbit polyclonal antiserum to OFV (*Anti-OFV*). The positions of the 55-kDa, 29-kDa and 23-kDa proteins are indicated on the *right*. The positions of the Fermentas marker proteins are shown on the *left*

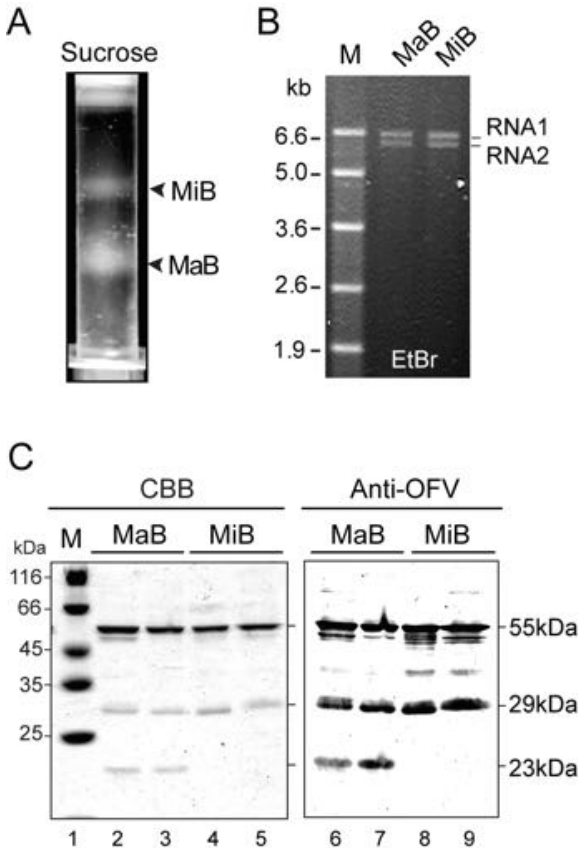

Fig. 3 RNA and protein components of two bands obtained in the OFV purification procedure. **A** OFV particles sedimenting as a major band (*MaB*) and a minor band (*MiB*) after ultracentrifugation in a 10−40% sucrose density gradient. **B** Agarose gel electrophoretic patterns of OFV RNAs extracted from MaB and MiB. The positions of viral RNA1 and RNA2 are indicated on the *right.* The positions of the Promega marker RNAs (*M*) are indicated on the *left.* **C** Detection of structural proteins in MaB and MiB by 12% SDS-PAGE (*CBB*) and Western blot analysis (*Anti-OFV*). The positions of the 55-kDa, 29-kDa and 23-kDa proteins are indicated on the *right*. The positions of the marker proteins are shown on the *left*

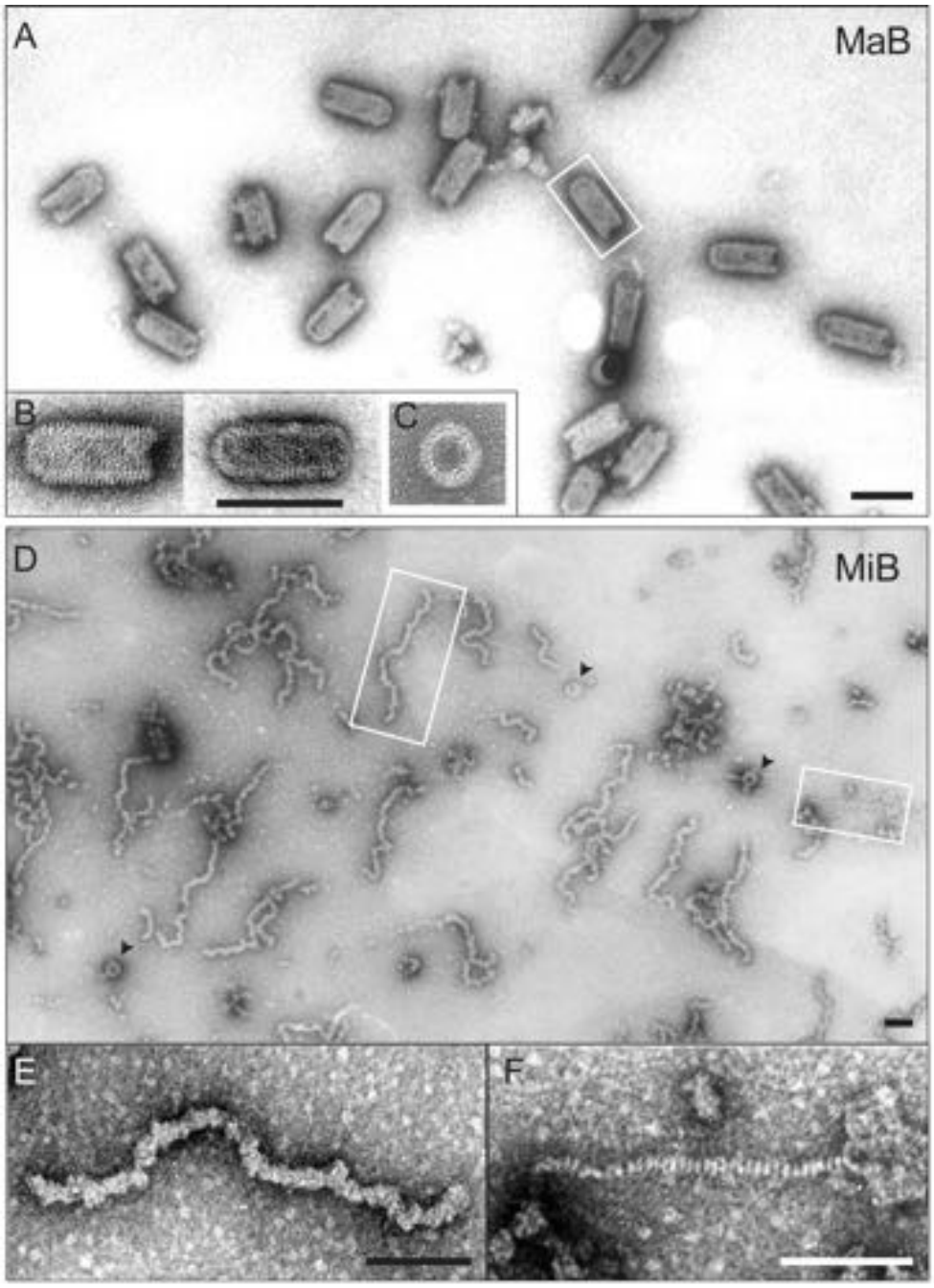

Fig. 4 Electron micrographs of the OFV particles separated by sucrose density gradient centrifugation. **A** Particles from the major band (*MaB*) in the sucrose gradient. **B** *Left*: an enlargement of the area outlined by the rectangle in (A). *Right*: a bacilliform particle from MaB. **C** A disk-like structure from MaB. **D** Particles from the minor band (*MiB*) in the gradient. *Arrowheads* indicate disk-like structures. **E** An enlargement of the left rectangle in (D). **f** An enlargement of the right rectangle in (D). All samples were stained with uranyl acetate. The *bar* represents 100 nm

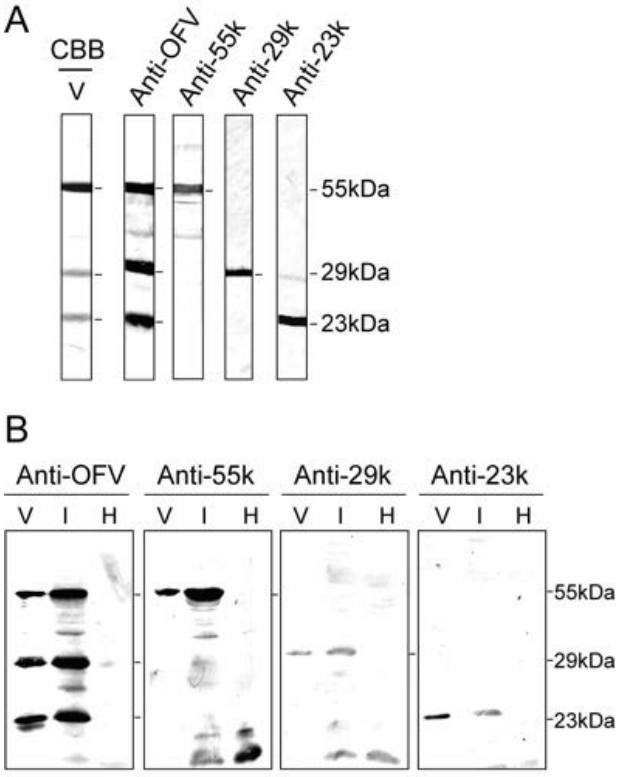

Fig. 5 Analysis of the structural proteins of OFV by using protein-specific antisera. **A** Western blot analysis of structural proteins of bullet-shaped particles. The preparative blot was cut into strips, which were then probed with rabbit antiserum to OFV virions (*Anti-OFV*) or mouse antisera to the 55-kDa (*Anti-55k*), 29-kDa (*Anti-29k*) or 23-kDa (*Anti-23k*) proteins. The positions of the viral proteins are indicated on the right. **B** Western blot detection of OFV proteins in an extract from infected *C. quinoa* leaves. Total proteins from the bullet-shaped particles (*V*), OFV-infected *C. quinoa* (*I*) and healthy *C. quinoa* (*H*) were resolved in 12% SDS-polyacrylamide gels and electroblotted onto nitrocellulose

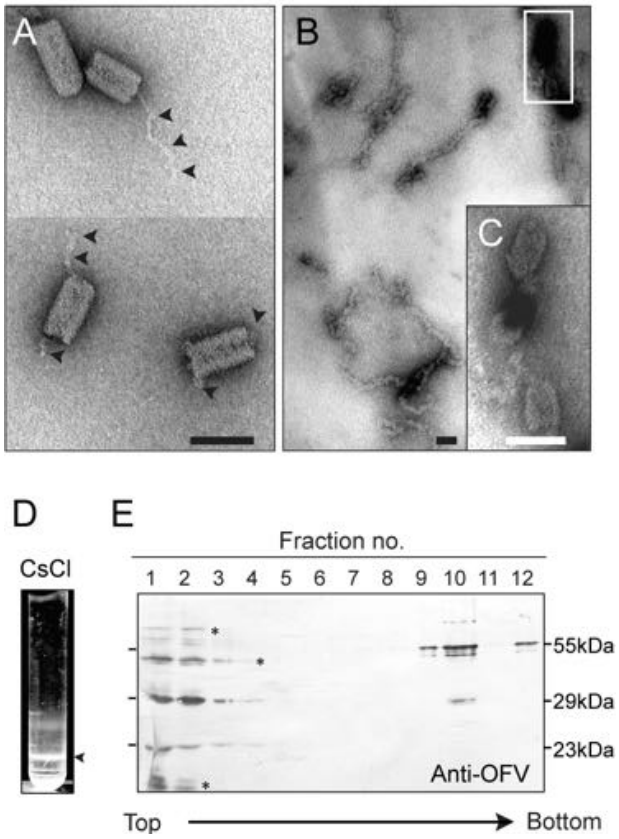

Fig. 6 Effect of NaCl and CsCl on stability of the OFV particles. **A** Transmission electron micrographs of the bullet-shaped particles treated with 2 % Triton X-100 plus 0.8M NaCl. *Arrowheads* indicate filamentous structures after partial disruption of OFV virions. **B** OFV particles obtained from the CsCl gradient. **C** An enlargement of the rectangle in (B). Samples were stained with uranyl acetate. The *bar* represents 100 nm. **D** Sedimentation pattern after a 20−40% (w/v) CsCl density gradient centrifugation. The *arrowhead* indicates the major band. **E** Western blot analysis with anti-OFV serum of 12 fractions from the top to the bottom of the CsCl gradient. Fraction 12 contained the resuspended pellet of the gradient. The positions of the 55-kDa, 29-kDa and 23-kDa proteins are indicated on the *right*. *Asterisks* indicate the putative degradation or aggregation products of the OFV proteins

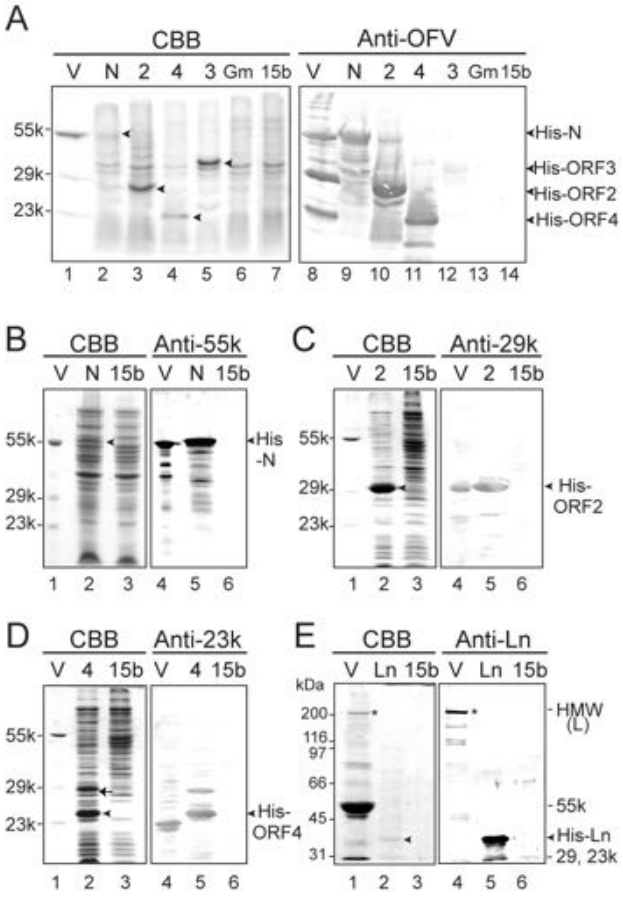

Fig. 7 Determination of ORFs in the OFV genome that encode structural proteins. **A**−**E** SDS-PAGE and Western blot analysis of prokaryotically expressed OFV proteins. Lysates of bacteria expressing N (ORF1) (*N*), ORF2 (*2*), ORF3 (*3*), ORF4 (*4*), G (ORF5) (*Gm*) and L (ORF6) (*Ln*) after induction with IPTG were fractionated in 12% (A−D) or 8% (E) SDS-PAGE and were stained with CBB. Total proteins from the bullet-shaped particles (*V*) and IPTG-induced bacteria containing the parental expression plasmid pET-15b (*15b*) were also analyzed. Proteins in gels were transferred to nitrocellulose and incubated with antisera to OFV virions (*Anti-OFV*), 55-kDa (*Anti-55k*), 29-kDa (*Anti-29k*), 23-kDa (*Anti-23k*), and Ln (*Anti-Ln*) proteins. *Arrowheads* indicate bacterially expressed recombinant proteins. *Arrow* indicates a different size band reacted with Anti-23k. The *asterisk* indicates the high molecular weight (*HMW*) protein. The positions of the viral and the HMW proteins are indicated on the *right*. The positions of the Bio-Rad marker proteins are indicated on the *left* (E)